Formability Limit Prediction of TRIP780 Steel Sheet Using Lode Angle Dependent Gurson-Based Models with Thomason Coalescence Criterion and Bifurcation Analysis

Muhammad Waqar Nasir[1,2, a)] Hocine Chalal[1, b)] Farid Abed-Meraim[1, c)]

[1] *Laboratory LEM3, Université de Lorraine, CNRS, Arts et Métiers ParisTech, F-57000 Metz, France.*
[2] *Department of Mechanical Engineering, University of Engineering and Technology, Lahore 54000, Pakistan.*

[a)] Corresponding author: muhammad_waqar.nasir@ensam.eu
[b)] hocine.chalal@ensam.eu
[c)] farid.abed-meraim@ensam.eu

Abstract. For biaxial stretching strain paths, which are typically encountered in sheet metal forming, the stress triaxiality ranges from 0.33 to 0.67. At this low level of triaxiality, voids change their shape from spherical to general spheroidal shape. In the literature, unit cell studies show the dependency of void shape on the lode parameter, especially at low stress triaxiality. Several authors also pointed out the influence of lode parameter on ductile failure. In the current study, lode parameter dependent Gurson-based models are combined with bifurcation analysis for the prediction of formability limits of TRIP780 steel sheet. Moreover, Thomason's coalescence criterion is considered for the prediction of critical porosity. For the anisotropic plastic behavior of the dense material, the quadratic Hill'48 yield surface is considered. Contribution to porosity evolution due to shear mechanism is also analyzed. In addition, the effect of lode parameter on the prediction of forming limit diagram (FLD) is investigated. It is observed that the accelerated evolution of porosity, due to the consideration of lode parameter, induces lower ductility limits for the modified Gurson-based model, as compared to the original Gurson model. The results also demonstrate that the use of the Thomason coalescence criterion for the determination of critical porosity plays an important role in the prediction of FLDs, as compared to fixed critical porosity used in the Gurson–Tvergaard–Needleman model.

INTRODUCTION

In manufacturing industry, one of the most-widely used processes is sheet metal forming process. For safer design of the manufactured parts, the latter must be free from any defects, such as localized necking, which is precursor to the material failure. Thus, accurate prediction of localized necking is a key point to select the optimized parameters for forming process. Formability limit diagram (FLD) is very useful and a practical tool to characterize the ductility limit of sheet metals in forming processes. However, the experimental determination of FLD is both costly and time consuming. Thanks to the recent developments of constitutive models as well as material instability criteria, the FLD can be predicted through numerical simulations.

The numerical prediction of the FLD is generally based on the coupling of constitutive models with material instability criteria. Rudnicki and Rice [1] and Rice [2] have shown that, in the framework of phenomenological constitutive models with associated plasticity and smooth yield surface, localization bifurcation cannot be predicted in the positive hardening regime. Therefore, softening regime is required in this situation, and can be introduced by coupling the phenomenological constitutive equations with damage. This can be undertaken using the well-known and widely-used micromechanics-based damage model proposed by Gurson [3]. In this model, the damage variable is defined as the ratio of volumes of the void and the representative volume element (RVE). The Gurson model has been subsequently modified to incorporate various physical phenomena, such as nucleation, coalescence, shape and size of voids, isotropic and kinematic hardening of the dense matrix material, etc. (see, e.g., [4–9]). In the original

Gurson model, it is assumed that both void and RVE are in spherical shape, while the void shape remains spherical even after plastic deformation. This assumption is valid for large stress triaxialities (see, e.g., Jackiewicz [10]). At low stress triaxialities, the shear components are significant and the void shape changes from spherical to general spheroidal. In the literature, the void shape evolution can be considered in Gurson-based models by introducing the lode parameter in the constitutive equations (see, e.g., [11,12]). Barsoum and Faleskog [13] showed through experimentation that, at low stress triaxialities, void shearing is the precursor to final rupture, while at high stress triaxialities, void growth is the dominating mechanism. Dunand and Mohr [14] and Kiran and Khandelwal [15] also showed through their simulations that the effect of lode parameter on the material failure is more prominent at low stress triaxialities than at higher ones. The effect of third stress invariant on the material behavior has been showed by several other authors (see, e.g., [16,17]). They outlined that the stress triaxiality alone is not sufficient to properly formulate the plastic yielding, and the third stress invariant must be included in the yield function. In the present study, the formability limits are investigated using shear modified Gurson-based models (see [12,18,19]), which are coupled with the Rice localization criterion (see, e.g., [2,20]).

The paper is organized as follows. First, the constitutive equations of the adopted shear modified Gurson-based models are briefly recalled. Then, the bifurcation condition following the Rice localization criterion is presented. The results related to the prediction of the FLD of TRIP780 steel sheet are presented and discussed. Finally, some concluding remarks are drawn.

CONSTITUTIVE EQUATIONS

In the present study, the shear modified Gurson-based model proposed by Nahshon and Hutchinson [18] is used. The associated plastic potential is similar to that of the Gurson–Tvergaard–Needleman (GTN) model [5], in which the evolution of porosity ($\dot{f}$) is defined as the sum of evolutions due to growth, nucleation, as well as a shear damage contribution:

$$\dot{f} = \dot{f}_g + \dot{f}_n + \dot{f}_s \,. \tag{1}$$

The evolution due to void growth is dependent upon hydrostatic plastic strain (see [21]). In this work, the strain-controlled nucleation as proposed by Chu and Needleman [4] is considered. Nahshon and Hutchinson [18] proposed a relation for the shear damage contribution that depends on the deviatoric part of the Cauchy stress tensor. The porosity evolution parts are given as:

$$\dot{f}_g = (1-f)\mathbf{D}^{\mathrm{p}} : \mathbf{I} \,, \tag{2}$$

$$\dot{f}_n = A_N \dot{\bar{\varepsilon}}^p \text{ with } A_N = \frac{f_N}{s_N\sqrt{2\pi}} exp\left(-\frac{1}{2}\left(\frac{\bar{\varepsilon}^p - \varepsilon_N}{s_N}\right)^2\right), \tag{3}$$

$$\dot{f}_s = k_w f\, \omega_0\left(\mathbf{\Sigma}\right)\frac{\mathbf{\Sigma}' : \mathbf{D}^{\mathrm{p}}}{\sigma_{eq}} \,, \tag{4}$$

where f_N, s_N, ε_N and k_w are material parameters, $\mathbf{I}$ is the second-order identity tensor, $\mathbf{D}^{\mathrm{p}}$ is the macroscopic plastic strain rate, $\bar{\varepsilon}^p$ is the cumulated equivalent plastic strain, $\mathbf{\Sigma}'$ is the deviatoric part of the Cauchy stress tensor $\mathbf{\Sigma}$. Nielsen and Tvergaard [19] suggested that the shear modification must be only valid for low triaxialities. Thus, a factor $\Omega(T)$ is defined such that the shear damage contribution becomes inactive beyond a specific threshold value of triaxiality T . The function $\omega_0\left(\mathbf{\Sigma}\right)$ in Eq. (4) is defined as:

$$\omega_0(\mathbf{\Sigma}) = \omega(\xi)\Omega(T) \text{ with } \Omega(T) = \left\{\begin{array}{cc} 1 & \text{for } T < T_1 \\ \dfrac{T-T_2}{T_1-T_2} & \text{for } T_1 \le T \le T_2 \\ 0 & \text{for } T > T_2 \end{array}\right\}, \tag{5}$$

where T_1 and T_2 are material parameters, while $\omega(\xi)$ is the shear scaling factor defined as:

$$\omega(\xi) = 1-\xi^2 \text{ with } \xi = \cos(3\theta) = \frac{27J_3}{2\sigma_{eq}^3} \text{ and } L = \sqrt{3}\tan(\theta - \frac{\pi}{6}) \,, \tag{6}$$

where θ is the angle formed between the deviatoric stress and the maximum principal stress in the deviatoric stress plane defined in the principal stress space (see [12]), L is the lode parameter, and J_3 is the third invariant of the deviatoric part of the Cauchy stress (i.e., $J_3 = \det(\mathbf{\Sigma}')$. It should be noted that for generalized tension, shear, and compression, the typical values for parameters L, θ and ξ are: $(L = -1; \theta = 0^{\circ}; \xi = 1)$, $(L = 0; \theta = 30^{\circ}; \xi = 0)$, and $(L = 1; \theta = 60^{\circ}; \xi = -1)$, respectively.

From finite element analysis on unit cell, Dæhli et al. [12] have pointed out that the shear damage term must be a monotonic decreasing function of lode parameter. Thus, they proposed a modified scaling factor $\omega(\xi) = (1+\xi)/2$ for the shear damage. For the biaxial loading paths, $\xi = -1$ corresponds to balanced biaxial tension, while $\xi = +1$ corresponds to uniaxial tension.

Elastic–Plastic Tangent Modulus and Numerical Implementation

The elastic–plastic tangent modulus for the resulting model is derived in this section. The expression of the plastic multiplier $\dot{\gamma}$ is first determined using the consistency condition, and then, the tangent modulus $\mathbf{C}^{\mathrm{ep}}$ is derived. Their expressions write:

$$\dot{\gamma} = \frac{\mathbf{V}_{\mathbf{\Sigma}} : \mathbf{C}^{\mathrm{e}} : \mathbf{D}}{\mathrm{H}_{\gamma}} \ , \tag{7}$$

$$\mathbf{C}^{\mathrm{ep}} = \mathbf{C}^{\mathrm{e}} - \frac{(\mathbf{C}^{\mathrm{e}} : \mathbf{V}_{\mathbf{\Sigma}}) \otimes (\mathbf{V}_{\mathbf{\Sigma}} : \mathbf{C}^{\mathrm{e}})}{\mathrm{H}_{\gamma}} \ , \tag{8}$$

where $\mathbf{V}_{\mathbf{\Sigma}}$ denotes the plastic flow direction, which is the partial derivative of the yield function with respect to the Cauchy stress $\mathbf{\Sigma}$, while $\mathbf{C}^{\mathrm{e}}$ is the fourth-order tensor of elastic constants. The expression of the denominator H_{γ} is not detailed here for conciseness (see [23]).

The resulting model is implemented into the static implicit FE code ABAQUS via a user material subroutine (UMAT). For each time increment, the elastic–plastic tangent modulus as well as the stress state are updated using and explicit time integration scheme, and more specifically, the fourth-order Runge–Kutta method.

Localization Bifurcation Criterion

To predict the ductility limit of sheet metals, the Rice criterion [2] for localized necking is considered in the present contribution. This criterion is based on the bifurcation analysis that corresponds to the loss of uniqueness of solution for the boundary value problem. According to this criterion, the condition of occurrence of localized necking writes:

$$\det(\mathbf{n} \cdot \mathbf{L} \cdot \mathbf{n}) = 0 \ , \tag{9}$$

where $\mathbf{n}$ is the normal to the localization band, while $\mathbf{L}$ is a fourth-order tangent modulus, which relates the nominal stress rate $\dot{\mathbf{N}}$ to the velocity gradient $\mathbf{G}$ (i.e., $\dot{\mathbf{N}} = \mathbf{L} : \mathbf{G}$). Using the Jaumann objective stress rate, it can be shown (see, e.g., Mansouri et al. [23]) that the fourth-order tangent modulus $\mathbf{L}$ is related to the elastic–plastic tangent modulus $\mathbf{C}^{\mathrm{ep}}$ through the following expression:

$$\mathbf{L} = \mathbf{C}^{\mathrm{ep}} + \mathbf{C}_1 - \mathbf{C}_2 - \mathbf{C}_3 \ , \tag{10}$$

where $\mathbf{C}_1$, $\mathbf{C}_2$ and $\mathbf{C}_3$ are convective terms, which are function of the Cauchy stress components (i.e., $C_{1ijkl} = \Sigma_{ij}\delta_{kl}$, $C_{2ijkl} = 0.5(\Sigma_{jk}\delta_{il} + \Sigma_{jl}\delta_{ik})$ and $C_{3ijkl} = 0.5(\Sigma_{ik}\delta_{jl} - \Sigma_{il}\delta_{jk})$. Since the plane-stress conditions are adopted in this work, the normal unit vector $(\mathbf{n})$ is searched only in the plane of the sheet metal. For each loading increment, the determinant of the acoustic tensor $(\mathbf{n} \cdot \mathbf{L} \cdot \mathbf{n})$ is computed. The numerical detection of strain localization is achieved when the minimum of the determinant of the acoustic tensor, over all possible normal vectors to the localization band, becomes non-positive.

Results and Discussion

In this section, both shear modified Gurson-based models of Nahshon and Hutchinson [18] and Dæhli et al. [12] are coupled with the Rice bifurcation criterion for the prediction of FLD of TRIP780 steel sheet. Note that, for both models, two coalescence criteria are considered for the determination of the critical porosity. The first one is based on a fixed critical porosity (see [5]), which is identified through an experimental procedure, while the second one (i.e., Thomason coalescence criterion [6]) assumes that the critical porosity is function of triaxiality. The material parameters of the TRIP780 steel sheet are taken from [24–26] and are summarized in Table 1.

TABLE 1. Material Properties for TRIP780 steel

E (GPa)	υ	r_0	r_{45}	r_{90}	K (MPa)	n	ε_0	q_1	q_2
185	0.3	0.881	1.002	1.197	1351	0.169	0.007	1	0.7
q_3	T_1	T_2	f_0	f_N	ε_N	s_N	k_w	f_{cr}	f_f
0.885	0.35	0.7	6×10^{-5}	0.045	0.25	0.1	2.4	0.067	0.08

The forming limit diagrams associated with the Nahshon and Hutchinson Gurson based-model [18] and the Dæhli et al. Gurson-based model [12] are reported in Fig.1, along with the experimental FLD for the same TRIP780 steel material taken from [26].

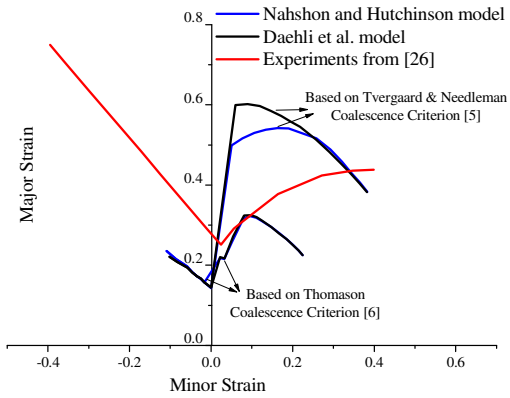

FIGURE 1. Forming Limit Diagram Using Rice's bifurcation criterion.

On the left-hand side of FLD, i.e. from uniaxial tension path to plane-strain tension path, the effect of the coalescence criterion on the ductility limits is very small for the Nahshon–Hutchinson model, which is also the case for the Dæhli et al. model. This is caused by the occurrence of strain localization before coalescence, in the left-hand side of FLD, as predicted by the Rice bifurcation criterion. On the right-hand side of FLD, i.e. from plane-strain tension path to balanced biaxial tension path, it is found that the ductility limits using the Thomason coalescence criterion are much lower than those obtained with the Tvergaard and Needleman coalescence criterion (i.e., fixed critical porosity) for both Nahshon–Hutchinson and Dæhli et al. models. Indeed, as the critical porosity obtained using the Thomason coalescence criterion is lower than the fixed one in Tvergaard and Needleman coalescence criterion (i.e., $f_{cr} = 0.067$, see Table 1), the coalescence regime is triggered earlier, thereby promoting early plastic flow localization. As to the lode angle dependent term $\omega(\xi)$, expression of the latter is different according to each of the two Gurson-based models. However, at balanced biaxial tension, both models provide the same lode angle dependent term, which leads to similar forming limits. On the whole, the predicted FLDs with both models are comparable, in terms of order of magnitude, to the experimental FLD provided in reference [26]. More specifically, with respect to the experimental results, the predicted limit strains are underestimated in the left-hand side of the FLD for both models and coalescence criteria. However, for both models in the right-hand side of the FLD, these limit strains are underestimated, respectively, overestimated when using the Thomason coalescence criterion and the

Tvergaard and Needleman coalescence criterion. This is probably due to the material parameter identification and, particularly, to the identification of damage parameters. Indeed, the latter are usually identified using only a uniaxial tension test at moderate strain levels, while accurate calibration of material parameters requires an identification procedure that is based on various types of mechanical tests at large strain levels. Moreover, the Rice bifurcation criterion, used in this work to predict the occurrence of localized necking, is based on the assumption of a homogeneous pre-localization state, with the only consideration of material instability, without taking into account any structural (geometric) effects. Consequently, the FLDs predicted by the present approach should be compared only qualitatively with the experimental FLD.

Effect of the Shear Parameter on FLD

In this section, the effect of the shear parameter k_w (see Eq. (4)) on the prediction of FLD is investigated. Note that, for $k_w = 0$, the contribution of shear damage to the evolution of porosity vanishes (see Eqs. (1) and (4)), which allows recovering the classical GTN model for both Nahshon–Hutchinson and Dæhli et al. models. Fig. 2 illustrates the sensitivity of the FLD to the shear damage parameter k_w for both investigated models and coalescence criteria. More specifically, for Thomason coalescence criterion, the effect of the shear parameter k_w on FLDs is small on the whole for both investigated models (see Figs. 2(a) and 2(b)), which is also the case for Tvergaard and Needleman coalescence criterion in the left-hand side of the FLDs (see Figs. 2(c) and 2(d)). However, the effect of the shear parameter is more perceptible in the right-hand side of the FLDs (see Figs. 2(c) and 2(d)), with larger values of shear parameter k_w inducing lower ductility limits.

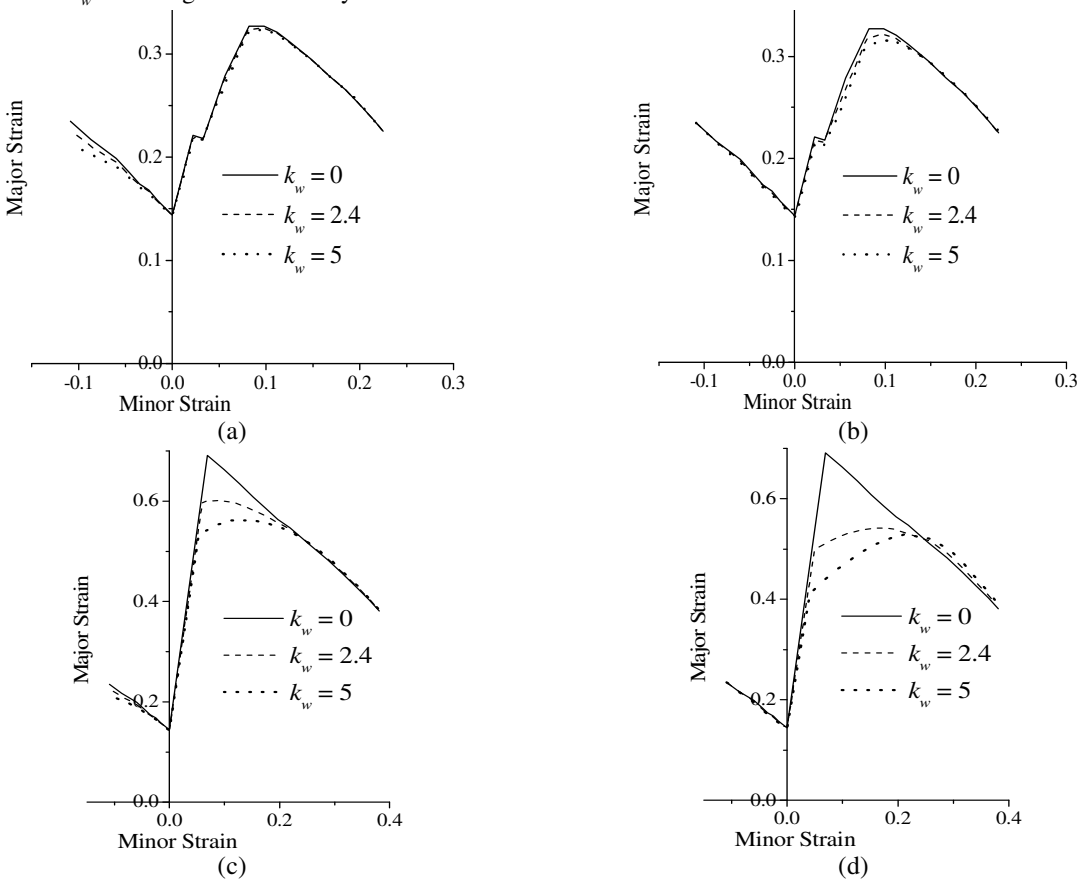

FIGURE 2. Shear parameter effects on FLD: (a) Dæhli et.al. model with Thomason coalescence criterion, (b) Nahshon-Hutchinson model with Thomason coalescence criterion, (c) Dæhli et.al. model with Tvergaard and Needleman coalescence criterion, (d) Nahshon-Hutchinson model with Tvergaard and Needleman coalescence criterion.

Conclusion

In this study, shear modified Gurson-based models, including the lode parameter, have been coupled with the Rice bifurcation criterion for the prediction of FLDs of TRIP780 steel material. Furthermore, the Thomason and Tvergaard and Needleman coalescence criteria have been considered for the determination of the critical porosity. The resulting models have been implemented into the FE code ABAQUS/Implicit via a user defined material subroutine (UMAT) in the framework of large strain and plane-stress analysis. From the numerical results, it is found that the Thomason coalescence criterion provides the lower values of critical porosity, as compared to the Tvergaard and Needleman coalescence criterion (i.e., fixed value of critical porosity). Therefore, the ductility limits associated with the Thomason coalescence criterion are lower than those using the Tvergaard and Needleman coalescence criterion. Although the shear damage parameter k_w has a strong influence on the material response, however, its effect on FLDs is small due to the low value of critical porosity obtained using the Thomason coalescence criterion, while more perceptible effect is observed in the right-hand side of FLDs in the case of Tvergaard and Needleman coalescence criterion.

REFERENCES

1. J.W. Rudnicki and J.R. Rice, J. Mech. Phys. Solids **23**, 371–394 (1975).
2. J.R. Rice, (1976). The localization of plastic deformation. In: Koiter (Ed.), *Theoretical and Applied Mechanics*, pp. 207–227.
3. A.L. Gurson, ASME J. Eng. Mater. Technol. **99**(1), 2–15 (1977).
4. C.C. Chu and A. Needleman, ASME J. Eng. Mater. Technol. **102**(3), 249–256 (1980).
5. V. Tvergaard and A. Needleman, Acta Metall. **32**(1), 157–169 (1984).
6. P.F. Thomason, Acta Metall. **33**(6), 1087–1095 (1985).
7. K. Madou and J.B. Leblond, J. Mech. Phys. Solids **60**(5), 1020–1036 (2012).
8. L. Morin, J.C. Michel and J.B. Leblond, Int. J. Solids Struct. **118**, 167–178 (2017).
9. M.E. Torki, C. Tekoğlu, J.B. Leblond and A.A Benzerga, Int. J. Plasticity **91**, 160–181 (2017).
10. J. Jackiewicz, Eng. Fract. Mech. **78**(3), 487–502 (2011).
11. X. Gao and J. Kim, Int. J. Solids Struct. **43**(20), 6277–6293 (2006).
12. L.E. Dæhli, D. Morin, T. Børvik and O.S. Hopperstad, Eng. Fract. Mech. **190**, 299–318 (2018).
13. I. Barsoum and J. Faleskog, Int. J. Solids Struct. **44**(6), 1768–1786 (2007).
14. M. Dunand and D. Mohr, J. Mech. Phys. Solids **66**, 133–153 (2014).
15. R. Kiran and K. Khandelwal, Eng. Fract. Mech. **128**, 121–138 (2014).
16. Y. Zhu, M.D. Engelhardt and R. Kiran, Eng. Fract. Mech. **199**, 410–437 (2018).
17. Y.S. Ma, D.Z. Sun, F. Andrieux and K.S. Zhang, Acta Mech. Solida Sin. **30**(5), 493–506 (2017).
18. K. Nahshon and J.W. Hutchinson, Eur. J. Mech. A. Solids **27**(1), 1–17 (2008).
19. K.L. Nielsen and V. Tvergaard, Eng. Fract. Mech. **77**(7), 1031–1047 (2010).
20. F. Abed-Meraim, T. Balan and G. Altmeyer, Int. J. Adv. Manuf. Tech **71**(5-8), 1247–1262 (2014).
21. V. Tvergaard, J. Mech. Phys. Solids **35**(1), 43–60 (1987).
22. R. Hill, Proc. R. Soc. Lond. A **193**(1033), 281–297 (1948).
23. L.Z. Mansouri, H. Chalal and F. Abed-Meraim, Mech. Mater. **76**, 64–92 (2014).
24. M. Dunand and D. Mohr, J. Mech. Phys. Solids **59**(7), 1374–1394 (2011).
25. D. Mohr, M. Dunand and K.H. Kim, Int. J. Plasticity **26**(7), 939–956 (2010).
26. S. Panich, F. Barlat, V. Uthaisangsuk, S. Suranuntchai and S. Jirathearanat, Mater. Design **51**, 756–766 (2013).